Inorganic Chemistry

Article

pubs.acs.org/IC

Electron-Transferred Donor/Acceptor Ferrimagnet with T_C = 91 K in a Layered Assembly of Paddlewheel [Ru_2] Units and TCNQ

Wataru Kosaka,[†,‡] Hiroki Fukunaga,[‡] and Hitoshi Miyasaka*[,†,‡]

[†]Institute for Materials Research, Tohoku University, 2-1-1 Katahira, Aoba-ku, Sendai 980-8577, Japan

[‡]Department of Chemistry, Graduate School of Science, Tohoku University, 6-3 Aramaki-Aza-Aoba, Aoba-ku, Sendai 980-8578, Japan

Supporting Information

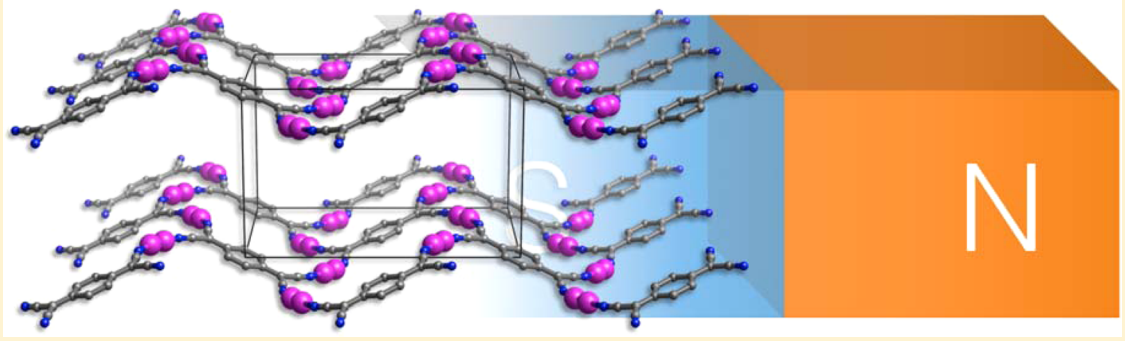

ABSTRACT: The donor (D)/acceptor (A) assembly reaction of the paddlewheel-type diruthenium(II,II) complex [Ru_2(2,4,6-F_3PhCO_2)$_4$(THF)$_2$] (2,4,6-$F_3PhCO_2^-$ = 2,4,6-trifluorobenzoate; abbreviated hereafter as [Ru_2]) with 7,7,8,8-tetracyano-*p*-quinodimethane (TCNQ) in a *p*-xylene/CH_2Cl_2 solvent system led to the formation of a two-dimensional layered compound, [{Ru_2(2,4,6-F_3PhCO_2)$_4$}$_2$(TCNQ)]·2(*p*-xylene)·2CH_2Cl_2 (**1**). As expected from this D/A combination, **1** has a one-electron-transfer ionic state with the $D^{0.5+}{}_2A^-$ formulation. This state formally derives a heterospin state composed of S = 1 for [$Ru^{II,II}{}_2$], S = $^3/_2$ for [$Ru^{II,III}{}_2$]$^+$, and S = $^1/_2$ for $TCNQ^{\bullet-}$, possibly causing intralayer ferrimagnetic spin ordering. Most of these types of compounds have an antiferromagnetic ground state because of the coupling of ferrimagnetically ordered layers in dipole antiferromagnetic interactions. However, **1** became a three-dimensional ferrimagnet with T_C = 91 K because of the presence of interlayer ferromagnetic interactions.

1. INTRODUCTION

Carboxylate-bridged paddlewheel diruthenium complexes (abbreviated hereafter as [Ru_2]) are useful building blocks (i.e., coordinating acceptor building blocks) for the construction of metal−organic frameworks (MOFs)[2,1] and are also suitable functional modules from which bulk functional materials with electronically or magnetically correlated characteristics can be designed.[3−7] A striking feature of [Ru_2] is its redox activity;[8,9] [Ru_2] is reversibly changeable between [$Ru^{II,II}{}_2$] and [$Ru^{II,III}{}_2$]$^+$,[10] which have different multiple spin states of S = 1 and $^3/_2$, respectively. Thus, [Ru_2] can alternate spin states without undergoing significant structural change.[8,9] Our group previously used a family of [$Ru^{II,II}{}_2$] complexes as electron-donor (D) building blocks for assembly reactions with polycyano organic acceptors (A) such as 7,7,8,8-tetracyano-*p*-quinodimethane (TCNQ)[11−14] and *N*,*N*′-dicyanoquinodiimine[15] derivatives to construct multidimensional MOFs composed of D and A building blocks (i.e., D/A-MOFs; TCNQ derivatives are hereafter abbreviated as $TCNQR_x$). Even in MOFs with coordinating frameworks, the D → A charge transfer and electron transfer can be controlled by combining the ionization potential of D and the electron affinity of A and also by utilizing the Madelung stability of electron-transferred ionic states.[2] We proposed that a family of benzoate-bridged paddlewheel [$Ru^{II,II}{}_2$] complexes should be useful for such modulars because their donation abilities can be finely tuned by introducing substituent groups in the phenyl group of benzoate.[10] In [Ru_2]$_2TCNQR_x$ compounds (i.e., D_2A-type compounds), two types of ionic states, the one-electron-transferred ionic state (1e-I; $D^+D^0A^-$ or $D^{0.5+}{}_2A^-$) and the two-electron transferred state (2e-I; $D^+{}_2A^{2-}$), may exist along with a neutral state (N; $D^0{}_2A^0$). Among these states, 1e-I is particularly intriguing because it can act as a magnet. To investigate this phenomenon, we have performed several assembly reactions based on combinations of benzoate-bridged [Ru_2] units and $TCNQR_x$ and demonstrated magnetic behavior with a relatively high T_C/T_N in a few 1e-I compounds with two-dimensional layered structures (T_C = Curie temperature; T_N = Néel temperature).[12b,d] However, the magnetic behavior in such low-dimensional layered systems is strongly affected by interlayer dipole interactions, which often cause antiferromagnetic coupling between the spins of different layers to converge to a singlet ground state[11b,d,12d] or generate random ordering,

Received: August 4, 2015
Published: September 28, 2015

DOI: 10.1021/acs.inorgchem.5b01776
Inorg. Chem. 2015, 54, 10001−10006

producing spin-glass-like magnets.[12b] In fact, only one example of a fine ferrimagnet has been previously reported (T_C = 66 K).[12d]

Herein we present a new fine ferrimagnet with T_C = 91 K in a $[Ru_2]_2$TCNQR$_x$ layered system. The new ferrimagnet has the formula $[\{Ru_2(2,4,6\text{-}F_3PhCO_2)_4\}_2(TCNQ)]\cdot 2(p\text{-xylene})\cdot 2CH_2Cl_2$ (**1**), where 2,4,6-$F_3PhCO_2^-$ = 2,4,6-trifluorobenzoate.

2. EXPERIMENTAL SECTION

General Procedures and Materials. All synthetic procedures were performed under an inert atmosphere using standard Schlenk-line techniques and a commercial glovebox. All chemicals were purchased from commercial sources and were of reagent grade. The solvents were dried using common drying agents and distilled under ultrapure nitrogen before use. The starting materials for the $[Ru^{II,II}_2]$ units were prepared by following previously reported methods.[10] Crystals of **1** contained some crystallization solvents, and some of them were slowly lost at room temperature (Figure S1), making the elemental analysis data difficult to interpret. Therefore, the samples were dried before elemental analysis (vide infra). The samples were aged as described above for a few hours after being removed from their mother liquids. Therefore, fresh samples picked up from the mother liquids were used for magnetic measurements.

Synthesis of ***1****.* A dichloromethane (CH_2Cl_2) solution (20 mL) of $[Ru_2(2,4,6\text{-}F_3PhCO_2)_4(THF)_2]$ (84 mg, 0.08 mmol) was divided into 1 mL aliquots, and each aliquot was placed in a narrow-diameter sealed glass tube (⌀ 8 mm) as the bottom layer. The middle layer, a mixture of *p*-xylene and CH_2Cl_2 [1:1 (v/v); 2 mL], was added carefully to the bottom layer. A 1 mL aliquot of a *p*-xylene solution (20 mL) of TCNQ (8.2 mg, 0.04 mmol) was carefully added on top of the middle layer in each tube. The glass tubes were left undisturbed in the glovebox for 1 month or more, after which block-shaped brownish-green crystals of **1** were obtained. X-ray crystallography and thermogravimetric measurements indicated that the crystals contained crystallization solvents [i.e., $2(p\text{-xylene})\cdot 2CH_2Cl_2$], which were partially eliminated after exposure to air (Figure S1). Hence, the samples used for elemental analysis were prepared by evacuation at room temperature for 4 h. Elem anal. Calcd for $[\{Ru_2(2,4,6\text{-}F_3PhCO_2)_4\}_2\{TCNQ\}]\cdot p\text{-xylene}$ ($C_{76}H_{30}N_4F_{24}O_{16}Ru_4$): C, 43.15; H, 1.42; N, 2.65. Found: C, 42.78; H, 1.69; N, 2.81. FT-IR (KBr, cm^{-1}): ν(C≡N) 2193, 2148.

General Physical Measurements. The IR spectra were measured on KBr disks with a Jasco FT-IR 620 spectrophotometer. Powder reflection spectra were measured on pellets diluted with $BaSO_4$ with a Shimadzu UV-3150 spectrometer. The magnetic susceptibility measurements were conducted with a Quantum Design SQUID magnetometer (MPMS-XL) in temperature and direct-current (dc) field ranges of 1.8−300 K and −7 to +7 T, respectively. Polycrystalline samples embedded in liquid paraffin were measured. The experimental data were corrected for the sample holder and liquid paraffin and for the diamagnetic contributions calculated from the Pascal constants.[16]

Crystallography. Single crystals with dimensions of 0.100 × 0.070 × 0.050 mm^3 were mounted on cryoloops using a Nujol and cooled by a stream of cooled dinitrogen gas. Measurements were made on a CCD diffractometer (Rigaku Mercury 70) with graphite-monochromated Mo Kα radiation (λ = 0.71070 Å). The structures were solved by direct methods (*SIR 92*)[17] and expanded using Fourier techniques (*DIRDIF99*).[18] All non-hydrogen atoms were refined anisotropically. Hydrogen atoms were introduced as fixed contributors. Full-matrix least-squares refinements of F^2 were based on observed reflections and variable parameters and converged with unweighted and weighted agreement factors of R1 = $\sum||F_o| - |F_c||/\sum|F_o|$ [$I > 2.00\sigma(I)$] and wR2 = $[\sum w(F_o^2 - F_c^2)^2/\sum w(F_o^2)^2]^{1/2}$ (all data). All calculations were performed using the *CrystalStructure* crystallographic software package.[19] The structural diagrams were prepared using *VESTA* software.[20] These data have been deposited as a CIF at the Cambridge Data Centre as supplementary publication no. 1416617. Copies of the data can be obtained free of charge by application to CCDC, 12 Union Road, Cambridge CB21EZ, U.K. (fax + 44-1223-336-033; e-mail deposit@ccdc.cam.ac.uk).

Crystallographic Data for ***1****:* $C_{86}H_{44}Cl_4F_{24}N_4O_{16}Ru_4$, M_r = 2391.36, monoclinic, $P2_1/c$ (No. 14), a = 12.277(2) Å, b = 18.378(3) Å, c = 21.067(4) Å, β = 106.845(2)°, V = 4549.3(13) Å^3, T = 93(1) K, Z = 2, D_{calc} = 1.746 g cm^{-3}, F_{000} = 2352.00, λ = 0.71070 Å, μ(Mo Kα) = 8.846 cm^{-1}, 35944 measured reflections, 10274 unique (R_{int} = 0.0201). R1 = 0.0390 [$I > 2\sigma(I)$], R1 = 0.0410 (all data), and wR2 = 0.1058 with GOF = 1.031.

3. RESULTS AND DISCUSSION

Syntheses and Characterization. Compound **1** was synthesized via a method similar to that used for other previously reported $[Ru_2]_2$TCNQ materials.[11,12] This method involves the slow diffusion of a donor, tetrahydrofuran (THF)-adducted $[Ru^{II,II}_2]$ complex (i.e., $[Ru^{II,II}_2(2,4,6\text{-}F_3PhCO_2)_4(THF)_2]$)[10] in CH_2Cl_2, and an acceptor, TCNQ in *p*-xylene, divided into bottom and top layers, respectively. Note that **1** can also be synthesized using another solvent system, toluene/CH_2Cl_2. However, because the obtained crystals were fragile because of the loss of interstitial solvents when the crystals were exposed to air, structural determination by single-crystal X-ray diffraction was unsuccessful.

The IR spectra of **1** exhibited characteristic ν(C≡N) stretches at 2193 and 2148 cm^{-1}. These bands were shifted to frequencies lower than those of the corresponding bands of neutral TCNQ (2222 cm^{-1}; Figure S2), indicating the reduced form of the TCNQ moiety. Powder reflection spectra of **1** measured on its pellet diluted with $BaSO_4$ show a wide range of absorption in the low-energy region of E < 1.5 eV, which is attributed to a few overlapping bands characteristic of the $D^{0.5+}{}_2A^-$ form as a π−π* transition on the TCNQ$^{\bullet-}$ moiety and charge-transfer bands between the $[Ru_2]$ and TCNQ$^{\bullet-}$ moieties and between $[Ru_2]$ units (Figure S3).[11d]

Structure of 1 and Evaluation of the Charge Distribution. Compound **1** was crystallized in the monoclinic $P2_1/c$ space group with Z = 2. An ORTEP drawing of the formula unit with an atom-numbering scheme is shown in Figure 1. The TCNQ moiety has an inversion center, whereas all atoms of one $[Ru_2]$ unit are crystallographically unique; half of the D_2A formula unit constitutes the asymmetric unit. The $[Ru_2]$ and TCNQ units act as a linear coordination acceptor and a μ_4-bridging coordination donor, respectively, to construct a fishnet-like, hexagonal, two-dimensional network, as found in similar D_2A systems (Figure 2a).[11a,b,d−f,12b,d,h] Relevant geometrical parameters are listed in Table 1. The two-dimensional network lies on the (100) plane to make a layer structure with an interlayer distance of 11.75 Å, as defined by the vertical distance between the planes (Figure 2b). The nearest interlayer TCNQ···TCNQ distance corresponds to the *a*-axis length (12.28 Å), while the corresponding $[Ru_2]\cdots[Ru_2]$ distance is 11.91 Å due to the waving feature of the D_2A layer (Figure 2b). Meanwhile, the $[Ru_2]\cdots[Ru_2]$ distances in the layer defined by the cis- and syn-coordinating positions of the TCNQ moiety are 10.71 and 10.16 Å, respectively (Figure 2a). The planes are stacked in an almost in-phase manner, with a tilt angle of θ = 16.8°, as defined by the vertical vector on the TCNQ plane and the shortest translation vector for TCNQ moieties between layers [i.e., $\theta = (\beta - 90)°$ for **1**, where β is the cell parameter β angle].[12b] Two *p*-xylene molecules as crystallization solvents are intercalated between the TCNQ moieties of the layers, as is often seen in D_2A layered systems (Figure S4),[11a,b,d−f,12b,21] and two CH_2Cl_2 molecules are located in the remaining void spaces between layers. The Ru−Ru bond distance is 2.2881(7) Å, slightly longer than that of $[Ru^{II,II}_2(2,4,6\text{-}$

DOI: 10.1021/acs.inorgchem.5b01776
Inorg. Chem. 2015, 54, 10001−10006

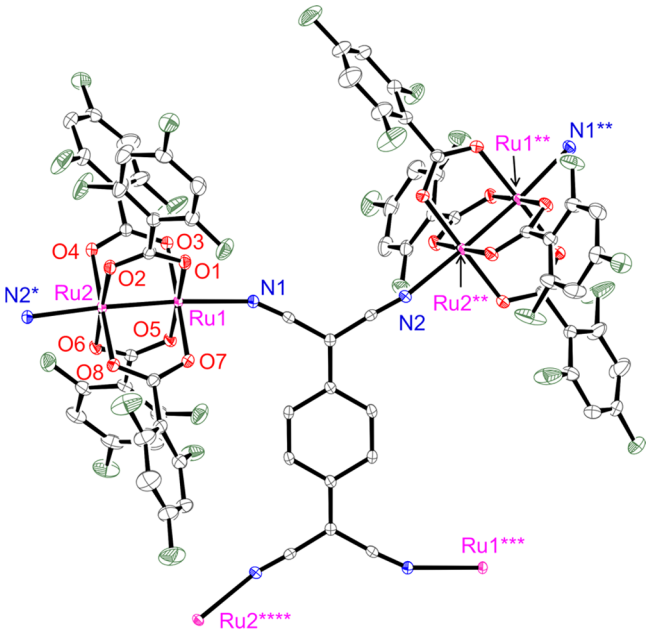

Figure 1. Thermal ellipsoid plot of the formula unit with an atom-numbering scheme for **1**, where oxygen, carbon, nitrogen, fluorine, and ruthenium are represented in red, gray, blue, green, and purple, respectively [50% probability ellipsoids; symmetry operations (*) x, $-y + {}^1/_2$, $z + {}^1/_2$; (**) x, $-y + {}^1/_2$, $z - {}^1/_2$; (***) $2 - x$, $1 - y$, $1 - z$; (****) $2 - x$, $y + {}^1/_2$, $-z + {}^3/_2$]. Crystallization solvents [2(*p*-xylene)·$2CH_2Cl_2$] and hydrogen atoms are omitted for clarity.

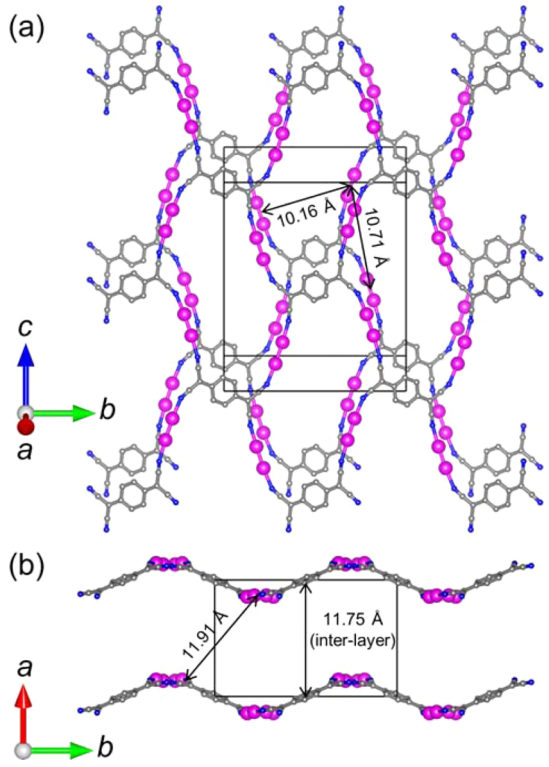

Figure 2. Packing diagrams projected along the (a) (100) plane and (b) c axis, where carbon, nitrogen, and ruthenium atoms are represented in gray, blue, and purple, respectively. Equatorial carboxylate ligands for $[Ru_2]$ units, crystallization solvents, and hydrogen atoms are omitted for clarity.

Table 1. Selected Bond Lengths (Å) and Angles (deg) in 1, Where θ Represents the Dihedral Angle between Least-Squares Planes Defined by the Phenyl Ring of the Benzoate Ligand and the Carboxylate-Bridging Mode (Atom Set of Ru_2O_2C)

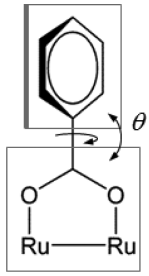

Bond Length (Å)	
Ru1−O1	2.0475(18)
Ru1−O3	2.048(2)
Ru1−O5	2.0540(18)
Ru1−O7	2.059(2)
Ru2−O2	2.0360(18)
Ru2−O4	2.047(2)
Ru2−O6	2.0474(18)
Ru2−O8	2.048(2)
Ru1−N1	2.238(3)
Ru2−N2[a]	2.232(2)
Ru1−Ru2	2.2881(7)
Ru2−Ru1−N1	175.75(6)
Ru1−Ru2−N2[a]	175.11(6)
Ru1−N1−C29	155.8(2)
Ru2[a]−N2−C31	163.7(2)
θ Angle (deg)	
benzoate set-1[b]	36.61
benzoate set-2[b]	38.98
benzoate set-3[b]	28.79
benzoate set-4[b]	56.25

[a]Symmetry codes: *, x, $-y + {}^1/_2$, $z + {}^1/_2$; **, x, $-y + {}^1/_2$, $z - {}^1/_2$. [b]Benzoate set-1 to -4: the phenyl group of C2−C7, C9−C14, C16−C21, and C23−C28, respectively.

$F_3PhCO_2)_4(THF)_2]$ [2.2723(2) Å].[10a] The average Ru−O_{eq} bond length (2.048 Å; O_{eq} = equatorial oxygen atoms), which is strongly influenced by the oxidation state of the $[Ru_2]$ core, is intermediate between those typically observed for $[Ru^{II,II}{}_2]$ (2.06−2.07 Å) and $[Ru^{II,III}{}_2]^+$ (2.02−2.03 Å),[8,9] indicating a partially oxidized feature, i.e., formally, $[Ru_2]^{0.5+}$ at least at the crystallographic analysis level.

Correspondingly, the oxidation state of $TCNQ^{\rho-}$ was assigned as 1− (i.e., a monoanion, $TCNQ^{\bullet-}$) based on the Kistenmacher relationship $\rho = A[c/(b + d)] + B$, with $A = -41.667$ and $B = 19.833$[22] evaluated based on neutral TCNQ ($\rho = 0$)[23] and RbTCNQ ($\rho = 1$)[24] (where b, c, and d are the TCNQ bond distances defined in Table 2). The estimated ρ value is 1.12, i.e., $\rho \approx 1$, which is in good agreement with the IR data and with the valence charges of the $[Ru_2]$ units, indicating a one-electron transfer from two $[Ru_2]$ units to one TCNQ with a formal oxidation state of $[\{Ru_2\}^{0.5+}-(TCNQ^{\bullet-})-\{Ru_2\}^{0.5+}]$.

Molecular Orbital Calculations of $[Ru^{II,II}{}_2]$ Units and Ionization Diagrams of the System. Recently, we proposed a simple method of predicting the electronic state of D/A-MOF to be either neutral (N) or ionic (I).[2] In this method, the

DOI: 10.1021/acs.inorgchem.5b01776
Inorg. Chem. 2015, 54, 10001−10006

Table 2. Comparison of the Bond Lengths (Å) in the TCNQ Moiety and a Charge of TCNQ (ρ) Estimated Based on Kistenmacher's Relationship[22]

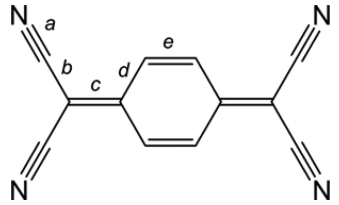

	charge	*a*	*b*	*c*	*d*	*e*	ρ[a]	ref
I[b]	0	1.140(1)	1.441(1)	1.374(3)	1.448(4)	1.346(3)	0	23
II[b]	1−	1.153(7)	1.416(8)	1.420(1)	1.423(3)	1.373(1)	−1	24
1		1.154(4)	1.410(4)	1.423(4)	1.416(4)	1.369(4)	−1.12[c]	this work
		1.152(4)	1.406(4)		1.427(4)			
		1.153[d]	1.408[d]		1.422[d]			

[a]Estimated from average values. [b]**I**: TCNQ.[23] **II**: RbTCNQ.[24] [c]$\rho = A_H[c/(b + d)] + B_H$, with $A_H = -41.667$ and $B_H = 19.833$.[22] [d]Average value.

energy gap between the highest occupied molecular orbital (HOMO) level of the D and the lowest unoccupied molecular orbital (LUMO) level of the A is evaluated as $E_{LUMO}(A) - E_{HOMO}(D) = \Delta E_{H-L}(DA)$; the N and I regimes are expected for $\Delta E_{H-L}(DA) > 0$ and $\Delta E_{H-L}(DA) < 0$, respectively.[2,12g] The calculated $E_{HOMO}(D)$ for the $[Ru_2(2,4,6\text{-}F_3PhCO_2)_4(THF)_2]$ unit and the $E_{LUMO}(A)$ for TCNQ are −4.7424 and −5.1215 eV, respectively;[2,10b,11d,e] thus, $\Delta E_{H-L}(DA)$ is −0.3791 eV, which suggests the formation of the ionic state in the assembled reaction between these components (Figure S5). Furthermore, we proposed another simple diagram to evaluate the boundary between the 1e-I (i.e., one-electron-transferred ionic state with $TCNQ^{\bullet-}$) and 2e-I (i.e., two-electron-transferred ionic state with $TCNQ^{2-}$) regimes by considering on-site Coulomb repulsion [$U = |^2E_{1/2}(A) - {}^1E_{1/2}(A)|$, where $^2E_{1/2}(A)$ and $^1E_{1/2}(A)$ are the second and first redox potentials of TCNQ, respectively].[2,11e,12g] In our previous study, we estimated the boundary energy level between the 1e-I and 2e-I regimes to be $-0.006405U + 2.9110$ eV and considered that $U = 582$ mV for TCNQ.[12g] Hence, the boundary energy level for TCNQ was predicted to be −0.8431 eV; i.e., the $\Delta E_{H\text{-}L}(DA)$ region from −0.8431 to 0 eV corresponds to the 1e-I regime (Figure S6), which is consistent with the observed 1e-I state in **1**.

Magnetic Properties. The temperature dependence of the magnetic susceptibility ($\chi = M/H$) of **1** was measured in a 1 kOe dc field in the temperature range from 1.82 to 300 K (cooling process). The χT product is plotted in Figure 3. The χT value of 2.86 $cm^3 \cdot K \cdot mol^{-1}$ at 300 K is much higher than that expected from the spin-only value of 2.00 $cm^3 \cdot K \cdot mol^{-1}$ for a set of two $S = 1$ spins with $g = 2.00$ for isolated [$Ru^{II,II}{}_2$] units calculated assuming a neutral state, which is consistent with the 1e-I state of **1** evaluated from the structure. Upon a decrease in the temperature, the χT value decreases slightly to a minimum of 2.84 $cm^3 \cdot K \cdot mol^{-1}$ at 280 K, gradually increases (e.g., 28.5 $cm^3 \cdot K \cdot mol^{-1}$ at 101 K), abruptly increases to reach 360 $cm^3 \cdot K \cdot mol^{-1}$ at 77 K, and finally decreases to 11.1 $cm^3 \cdot K \cdot mol^{-1}$ at 1.8 K. The minimum χT in the higher-temperature region indicates a strongly coupled ferrimagnetic spin arrangement in a layer, and the abrupt increase of χT at around 100 K is due to long-range magnetic ordering, as defined by the magnetization (or susceptibility) behavior at lower temperatures (vide infra).[11b,d,12d] The χ value measured at 1 kOe exhibits a rapid increase at 90−100 K without any subsequent decrease, even at low temperatures. This behavior is essentially the same in the field-cooled magnetization (FCM) curves measured at lower

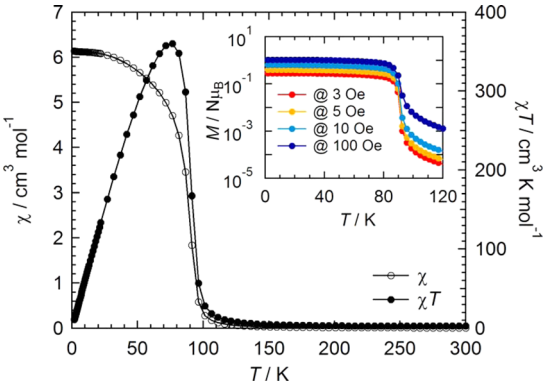

Figure 3. Temperature dependence of χ and χT for **1** measured under a dc field of 1 kOe. Inset: FCM curves of **1** measured under dc fields of 3, 5, 10, and 100 Oe.

fields of 3−100 Oe (inset of Figure 3), demonstrating the onset of ferrimagnetic long-range ordering at around 100 K.

To thoroughly investigate the long-range spin ordering, the temperature dependence of the alternating-current (ac) magnetic susceptibility (χ', real part; χ'', imaginary part) was measured under zero dc field with a 3 Oe oscillating field in the frequency range from 1 to 1.5 kHz (Figure 4). The χ' value

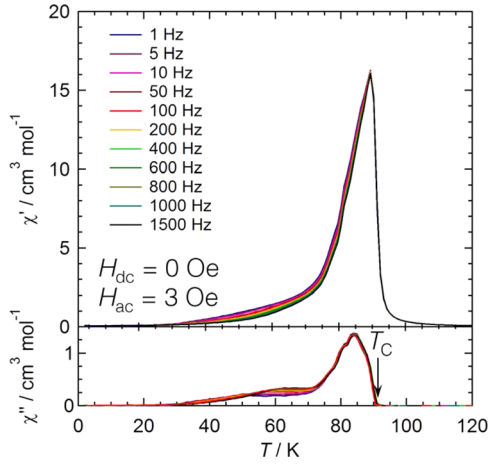

Figure 4. Temperature dependence of the ac magnetic susceptibilities χ' (in-phase) and χ'' (out-of-phase) at zero dc field and 3 Oe ac oscillating field for **1**.

DOI: 10.1021/acs.inorgchem.5b01776
Inorg. Chem. 2015, 54, 10001−10006

exhibits a single distinct peak at 89 K without any noticeable frequency dependence at the maximum accompanied by an increase in χ'' at 91 K, indicating the onset of long-range ferrimagnetic ordering with T_C = 91 K. The χ' and χ'' features at around 30−70 K, which appear similar to those of the existing multirelaxation processes, could be associated with the dynamic behaviors of domains with various sizes and/or of a small size of domains triggered at structural defects.

The field dependence of the magnetization was measured for fields ranging from −7 to +7 T at various temperatures ranging from 1.8 to 100 K (Figure 5). The field sweeps between +7 T and −7 T at given temperatures reveal the field hysteresis of the magnetization; the coercive field (H_c) and remnant magnetization (RM) are plotted as functions of temperature in the inset of Figure 5. The H_c value at 1.8 K is 9.2 kOe, which is on the same order as those of similar ferrimagnetic layered compounds [{Ru_2(*x*-$FPhCO_2$)$_4$BTDA-TCNQ} [*x*-$FPhCO_2^-$ = *x*-fluorobenzoate, BTDA-TCNQ = bis[1,2,5]-thiadizolotetracyanoquinodimethane; *x* = *o*-, H_c = 5 kOe; *x* = *p*-, H_c = 5.8 kOe];[12b] however, this value is smaller than those found in field-induced ferrimagnets that are derived by modifying antiferromagnets by applying fields, [{$Ru_2(CF_3CO_2)_4$}$_2$TCNQF_4] ($CF_3CO_2^-$ = trifluorobenzoate; TCNQF_4 = 2,3,5,6-tetrafluoro-7,7,8,8-tetracyanoquinodimethane; H_c > 2 T)[11b,d] and [{Ru_2(*o*-$ClPhCO_2$)$_4$}$_2$TCNQ(MeO)$_2$] [*o*-$ClPhCO_2^-$ = *o*-chlorobenzoate; TCNQ(MeO)$_2$ = 2,5-dimethoxy-7,7,8,8-tetracyanoquinodimethane; H_c = 1.6 T].[12d] This difference may be associated with magnetic anisotropy on spin ordering, as well as the interlayer interaction. The coercive field quasi-exponentially decreases with increasing temperature and finally disappears at around 90 K, corresponding to T_C. The RM begins to decrease at temperatures above 60 K. In the high-field region of 2−7 T, the magnetization increases linearly to reach 1.62 μ_B at 7 T and 1.8 K, but it does not saturate, even at 7 T. This behavior is generally observed for magnetic materials containing [$Ru^{II,II}_2$] or [$Ru^{II,III}_2$] units and is attributed to the strong intrinsic anisotropy of the constituent [Ru_2] units ($D \sim 270$ cm^{-1} for [$Ru^{II,II}_2$] with S = 1 and $D \sim 70$ cm^{-1} for [$Ru_2^{II,III}$]$^+$ with S = $^3/_2$)[3,4,8,9] along with the structural anisotropy expected for layered magnets.

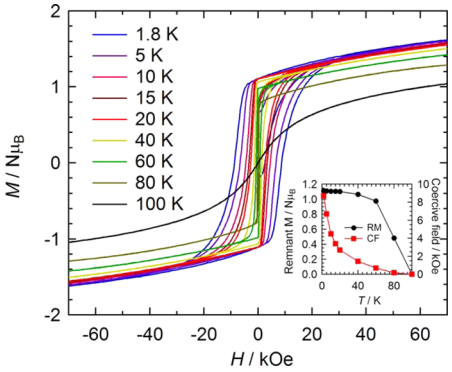

Figure 5. Field dependence of the magnetization of **1** at several temperatures between 1.8 and 100 K. Inset: temperature dependence of the RM at H = 0 and coercive field H_C.

4. CONCLUSION

A new D/A two-dimensional layered assembly, [{Ru_2(2,4,6-F_3PhCO_2)$_4$}$_2$(TCNQ)]·2(*p*-xylene)·2CH_2Cl_2 (**1**), was synthesized. The electronic state of **1** was assigned as the one-electron-transferred ionic state, which was found to be charge-delocalized as [{Ru_2}$^{0.5+}$−TCNQ$^{\bullet-}$−{Ru_2}$^{0.5+}$] from a structural point of view. Strong antiferromagnetic coupling between the spins of [$Ru^{II,II}_2$] (S = 1), [$Ru^{II,III}_2$]$^+$ (S = $^3/_2$), and TCNQ$^{\bullet-}$ (S = $^1/_2$) was observed within a layer, inducing intralayer ferrimagnetic ordering. Furthermore, interlayer ferromagnetic coupling was found in **1**, which finally induced three-dimensional ferrimagnetic ordering at T_C = 91 K. Such layered systems as fine ferrimagnets are still scarce; this system is the second example in the series of D_2A systems made from [Ru_2] units and TCNQR_x. The most intriguing result is that **1** has a relatively high transition temperature of T_C = 91 K, despite its low-dimensional system. Of course, the type of magnetic ordering, i.e., antiferromagnetic or ferrimagnetic, is dependent on the interlayer interactions, which are strongly affected by the interlayer environments and packing features of the layers.[12b,d] Thus, controlling the interlayer magnetic interactions (e.g., by inserting paramagnetic species[14] or guest molecules) would be an efficient strategy to design magnets with high T_C.

■ ASSOCIATED CONTENT

Supporting Information

The Supporting Information is available free of charge on the ACS Publications website at DOI: 10.1021/acs.inorgchem.5b01776.

IR spectra, figures for structure, and ionization diagrams (PDF)

CIF files giving X-ray crystallographic data for **1** (CIF)

■ AUTHOR INFORMATION

Corresponding Author

*E-mail: miyasaka@imr.tohoku.ac.jp. Tel: +81-22-215-2030. Fax: +81-22-215-2031.

Notes

The authors declare no competing financial interest.

■ ACKNOWLEDGMENTS

The authors thank Dr. Natsuko Motokawa and Ryo Atsuumi (Tohoku University) for their helpful contributions to the synthesis and magnetic measurements. This work was supported by Grants-in-Aid for Scientific Research (Grants 15K13652 and 26810029) and a Grant-in-Aid for Scientific Research on Innovative Areas ("π-System Figuration" Area 2601; Grant 15H00983) from the MEXT of Japan, ICC-IMR project, LC-IMR project, E-IMR project, Asahi Glass Foundation, and Mitsubishi Foundation. H.F. is thankful for support from the Tohoku University Institute for Promoting Graduate Degree Programs Division for International Advanced Research and Education.

■ REFERENCES

(1) Miyasaka, H. *Acc. Chem. Res.* **2013**, *46*, 248−257.

(2) (a) Kosaka, W.; Yamagishi, K.; Yoshida, H.; Matsuda, R.; Kitagawa, S.; Takata, M.; Miyasaka, H. *Chem. Commun.* **2013**, *49*, 1594−1596. (b) Kosaka, W.; Yamagishi, K.; Hori, A.; Sato, H.; Matsuda, R.; Kitagawa, S.; Takata, M.; Miyasaka, H. *J. Am. Chem. Soc.* **2013**, *135*, 18469−18480. (c) Kosaka, W.; Yamagishi, K.; Matsuda, R.; Kitagawa, S.; Takata, M.; Miyasaka, H. *Chem. Lett.* **2014**, *43*, 890−892. (d) Kosaka, W.; Yamagishi, K.; Zhang, J.; Miyasaka, H. *J. Am. Chem. Soc.* **2014**, *136*, 12304−12313.

(3) Aquino, M. A. S. *Coord. Chem. Rev.* **2004**, *248*, 1025−1045.

DOI: 10.1021/acs.inorgchem.5b01776
Inorg. Chem. 2015, 54, 10001−10006

(4) Mikuriya, M.; Yoshioka, D.; Handa, M. *Coord. Chem. Rev.* **2006**, *250*, 2194−2211.
(5) (a) Wang, X.-Y.; Avendaño, C.; Dunbar, K. R. *Chem. Soc. Rev.* **2011**, *40*, 3213−3238. (b) Miller, J. S. *Chem. Soc. Rev.* **2011**, *40*, 3266−3296. (c) Miller, J. S. *Dalton Trans.* **2006**, 2742−2749.
(6) (a) Liao, Y.; Shum, W. W.; Miller, J. S. *J. Am. Chem. Soc.* **2002**, *124*, 9336−9337. (b) Vos, T. E.; Liao, Y.; Shum, W. W.; Her, J.-H.; Stephens, P. W.; Reiff, W. M.; Miller, J. S. *J. Am. Chem. Soc.* **2004**, *126*, 11630−11639. (c) Vos, T. E.; Miller, J. S. *Angew. Chem., Int. Ed.* **2005**, *44*, 2416−2419. (d) Miller, J. S.; Vos, T. E.; Shum, W. W. *Adv. Mater.* **2005**, *17*, 2251−2254. (e) Miller, J. S. *CrystEngComm* **2005**, *7*, 458−461. (f) Liu, W.; Nfor, E. N.; Li, Y.-Z.; Zuo, J.-L.; You, X.-Z. *Inorg. Chem. Commun.* **2006**, *9*, 923−925. (g) Shum, W. W.; Her, J.-H.; Stephens, P. W.; Lee, Y.; Miller, J. S. *Adv. Mater.* **2007**, *19*, 2910−2913. (h) Shum, W. W.; Schaller, J. N.; Miller, J. S. *J. Phys. Chem. C* **2008**, *112*, 7936−7938. (i) Kennon, B. S.; Her, J.-H.; Stephens, P. W.; Miller, J. S. *Inorg. Chem.* **2009**, *48*, 6117−6123. (j) Fishman, R. S.; Okamoto, S.; Miller, J. S. *Phys. Rev. B: Condens. Matter Mater. Phys.* **2009**, *80*, 140416. (k) Kennon, B. S.; Stone, K. H.; Stephens, P. W.; Miller, J. S. *CrystEngComm* **2009**, *11*, 2185−2191. (l) Kennon, B. S.; Miller, J. S. *Inorg. Chem.* **2010**, *49*, 5542−5545. (m) Kennon, B. S.; Stone, K. H.; Stephens, P. W.; Miller, J. S. *Inorg. Chim. Acta* **2010**, *363*, 2137−2143. (n) Fishman, R. S.; Shum, W. W.; Miller, J. S. *Phys. Rev. B: Condens. Matter Mater. Phys.* **2010**, *81*, 172407. (o) DaSilva, J. G.; Miller, J. S. *Inorg. Chem.* **2013**, *52*, 1418−1423. (p) Haque, F.; del Barco, E.; Fishman, R. S.; Miller, J. S. *Polyhedron* **2013**, *64*, 73−76. (q) O'Neal, K. R.; Liu, Z.; Miller, J. S.; Fishman, R. S.; Musfeldt, J. L. *Phys. Rev. B: Condens. Matter Mater. Phys.* **2014**, *90*, 104301. (r) Stone, K. H.; Stephens, P. W.; Wainer, M. B.; Davidson, R. A.; Miller, J. S. *Inorg. Chim. Acta* **2015**, *424*, 116−119.
(7) Miyasaka, H.; Asai, Y.; Motokawa, N.; Kubo, K.; Yamashita, M. *Inorg. Chem.* **2010**, *49*, 9116−9118.
(8) Cotton, F. A.; Walton, R. A. *Multiple Bonds between Metal Atoms*, 2nd ed.; Oxford University Press: Oxford, U.K., 1993.
(9) Aquino, M. A. S. *Coord. Chem. Rev.* **1998**, *170*, 141−202.
(10) (a) Miyasaka, H.; Motokawa, N.; Atsuumi, R.; Kamo, H.; Asai, Y.; Yamashita, M. *Dalton Trans.* **2011**, *40*, 673−682. (b) Kosaka, W.; Itoh, M.; Miyasaka, H. *Dalton Trans.* **2015**, *44*, 8156−8168.
(11) (a) Miyasaka, H.; Campos-Fernández, C. S.; Clérac, R.; Dunbar, K. R. *Angew. Chem., Int. Ed.* **2000**, *39*, 3831−3835. (b) Miyasaka, H.; Izawa, T.; Takahashi, N.; Yamashita, M.; Dunbar, K. R. *J. Am. Chem. Soc.* **2006**, *128*, 11358−11359. (c) Motokawa, N.; Oyama, T.; Matsunaga, S.; Miyasaka, H.; Sugimoto, K.; Yamashita, M.; Lopez, N.; Dunbar, K. R. *Dalton Trans.* **2008**, 4099−4102. (d) Miyasaka, H.; Motokawa, N.; Matsunaga, S.; Yamashita, M.; Sugimoto, K.; Mori, T.; Toyota, N.; Dunbar, K. R. *J. Am. Chem. Soc.* **2010**, *132*, 1532−1544. (e) Nakabayashi, K.; Nishio, M.; Kubo, K.; Kosaka, W.; Miyasaka, H. *Dalton Trans.* **2012**, *41*, 6072−6074. (f) Nishio, M.; Motokawa, N.; Takemura, M.; Miyasaka, H. *Dalton Trans.* **2013**, *42*, 15898−15901.
(12) (a) Motokawa, N.; Miyasaka, H.; Yamashita, M.; Dunbar, K. R. *Angew. Chem., Int. Ed.* **2008**, *47*, 7760−7763. (b) Motokawa, N.; Oyama, T.; Matsunaga, S.; Miyasaka, H.; Yamashita, M.; Dunbar, K. R. *CrystEngComm* **2009**, *11*, 2121−2130. (c) Motokawa, N.; Miyasaka, H.; Yamashita, M. *Dalton Trans* **2010**, *39*, 4724−4726. (d) Motokawa, N.; Matsunaga, S.; Takaishi, S.; Miyasaka, H.; Yamashita, M.; Dunbar, K. R. *J. Am. Chem. Soc.* **2010**, *132*, 11943−11951. (e) Miyasaka, H.; Morita, T.; Yamashita, M. *Chem. Commun.* **2011**, *47*, 271−273. (f) Fukunaga, H.; Kosaka, W.; Miyasaka, H. *Chem. Lett.* **2014**, *43*, 541−543. (g) Kosaka, W.; Morita, T.; Yokoyama, T.; Zhang, J.; Miyasaka, H. *Inorg. Chem.* **2015**, *54*, 1518−1527. (h) Fukunaga, H.; Yoshino, T.; Sagayama, H.; Yamaura, J.; Arima, T.; Kosaka, W.; Miyasaka, H. *Chem. Commun.* **2015**, *51*, 7795−7798.
(13) (a) Nishio, M.; Hoshino, N.; Kosaka, W.; Akutagawa, T.; Miyasaka, H. *J. Am. Chem. Soc.* **2013**, *135*, 17715−17718. (b) Nishio, M.; Miyasaka, H. *Inorg. Chem.* **2014**, *53*, 4716−4723.
(14) Fukunaga, H.; Miyasaka, H. *Angew. Chem., Int. Ed.* **2014**, *54*, 569−573.
(15) (a) Miyasaka, H.; Motokawa, N.; Chiyo, T.; Takemura, M.; Yamashita, M.; Sagayama, H.; Arima, T. *J. Am. Chem. Soc.* **2011**, *133*, 5338−5345. (b) Nakabayashi, K.; Miyasaka, H. *Chem. - Eur. J.* **2014**, *20*, 5121−5131.
(16) Boudreaux, E. A.; Mulay, L. N. *Theory and Applications of Molecular Paramagnetism*; John Wiley and Sons: New York, 1976; p 491.
(17) Altomare, A.; Burla, M. C.; Camalli, M.; Cascarano, M.; Giacovazzo, C.; Guagliardi, A.; Polidori, G. *J. Appl. Crystallogr.* **1994**, *27*, 435−436.
(18) Beurskens, P. T.; Admiraal, G.; Beurskens, G.; Bosman, W. P.; de Gelder, R.; Israel, R.; Smits, J. M. M. *The DIRDIF-99 program system*; Technical Report of the Crystallography Laboratory; University of Nijmengen: Nijmengen, The Netherlands, 1999.
(19) *CrystalStructure 3.15: Crystal Structure Analysis Package*; Rigaku and Rigaku/MSC: The Woodlands TX, 2000−2002.
(20) Momma, K.; Izumi, F. *J. Appl. Crystallogr.* **2008**, *41*, 653−658.
(21) Nozaki, T.; Kosaka, W.; Miyasaka, H. *CrystEngComm* **2012**, *14*, 5398−5401.
(22) Kistenmacher, T. J.; Emge, T. J.; Bloch, A. N.; Cowan, D. O. *Acta Crystallogr., Sect. B: Struct. Crystallogr. Cryst. Chem.* **1982**, *38*, 1193−1199.
(23) Long, R. E.; Sparks, R. A.; Trueblood, K. N. *Acta Crystallogr.* **1965**, *18*, 932−939.
(24) Fritchie, C. J., Jr.; Arthur, P., Jr. *Acta Crystallogr.* **1966**, *21*, 139−145.

DOI: 10.1021/acs.inorgchem.5b01776
Inorg. Chem. 2015, 54, 10001−10006